Mammalian Genome 11, 8–15 (2000).

Mammalian Genome
Incorporating Mouse Genome

An axonemal dynein at the *Hybrid Sterility 6* locus: implications for *t* haplotype-specific male sterility and the evolution of species barriers

John Fossella,[1] Sadhana A. Samant,[2] Lee M. Silver,[1] Stephen M. King,[3] Kevin T. Vaughan,[4] Patricia Olds-Clarke,[2] Karl A. Johnson,[5] Atsushi Mikami,[6] Richard B. Vallee,[6] Stephen H. Pilder[2]

[1]Department of Molecular Biology, Princeton University, Princeton, New Jersey 08540, USA
[2]Department of Anatomy and Cell Biology, Temple University School of Medicine, 3400 N. Broad St., Philadelphia, Pennsylvania 19140, USA
[3]Department of Biochemistry, University of Connecticut Health Center, Farmington, Connecticut 06032-3305, USA
[4]Department of Biological Sciences, University of Notre Dame, Notre Dame, Indiana 46556, USA
[5]Department of Biology, Haverford College, Haverford, Pennsylvania 19041, USA
[6]Department of Cell Biology, University of Massachusetts Medical School, Worcestire, Massachusetts 01605, USA

Received: 13 July 1999 / Accepted: 25 August 1999

Abstract. Poor sperm motility characterized by a distinct aberration in flagellar waveform known as "curlicue" is a hallmark of *t* haplotype (*t*) homozygous male sterility. Previous studies have localized "curlicue" and a flagellar developmental defect, "whipless", to the *Hybrid Sterility 6* locus (*Hst6*), between the markers *Pim1* and *Crya1*. More recent heterospecific breeding experiments between *Mus spretus* (*Spretus*) and *Mus musculus domesticus* (*Domesticus*) have mapped the primary source(s) of both "curlicue" and "whipless" to a small sub-locus of *Hst6*, Curlicue a (*Ccua*). Here we report the complete physical isolation of the *Ccua* locus and the identification of a candidate gene for expression of both "whipless" and "curlicue" at its proximal end, an axonemal dynein heavy chain gene, *Dnahc8*, formerly mapped by interspecific backcross analysis near *Pim1*. *Dnahc8* mRNA expression commences in the *Domesticus* wild-type testis just prior to flagellar assembly and is testis-specific in the adult male. However, expression of *Dnahc8* is not readily evident in the testis of either *Spretus* or "whipless" animals (*Domesticus* males homozygous for the *Spretus* allele of *Dnahc8*). Our results argue that *Dnahc8* is fundamental to flagellar organization and function in *Domesticus*, but not *Spretus*, and suggest that *Dnahc8* is integral to both *Hst6*- and *t*-specific male infertility.

Introduction

t Haplotypes are structural variants of the proximal third of Chromosome (Chr) 17 found in most natural populations of the house mouse (*Mus musculus* and its various subspecies). The alteration in *t* genomic organization is characterized by four large nonoverlapping inversions relative to the wild-type (+) homolog, so that recombination across the entire 30–40 Mb *t* region (also called the *t* complex) is almost completely suppressed in +/*t* heterozygotes (Fig. 1; Silver and Artzt 1981; Hammer et al. 1989). As a result, numerous mutations, many affecting male reproduction, have accumulated and become fixed in *t* haplotypes.

All homozygous *t*/*t* males are sterile. Thus, the persistence of *t* variants in natural populations of commensal mice relies on their ability to transmit themselves from +/*t* heterozygous males at relatively high (non-Mendelian) ratios. Interestingly, +/*t* male meiotic drive (or transmission ratio distortion) and *t*/*t* male sterility may have a common genetic basis (Lyon 1984, 1986). Heterozygous +/*t* male meiotic drive supposedly derives from the interaction of at least three *t* complex inversion-specific distorter/sterility factors (*Tcd* /*Tcs1, 2, 3*, etc., *Tcd* /*Tcs2* having the strongest effect on both meiotic drive and male sterility) with a centrally located *t* complex responder (*Tcr;* Fig. 1). Hypothetically, the transmission ratio advantage of sperm carrying *t* in +/*t* heterozygous males is determined by the relative abilities of the Tcr^t and Tcr^t alleles to interact with either the deleterious *Tcd* /Tcs^+ alleles or their normal wild-type counterparts (Lyon 1984). However, the *Tcr*-independent nature of the male sterility phenotype exhibited by *t*/*t* homozygotes appears to be the consequence not only of the detrimental activity of homozygous *Tcd* /Tcs^t factors, but the absence of required "complementing" *Tcd* /Tcs^+ activity, as well (Lyon 1986; Olds-Clarke and Johnson 1993).

While the molecular nature of *t*-specific male traits is undoubtedly complex (Redkar et al. 1998; Samant et al. 1999; Silver and Buck 1993; Silver 1993), numerous studies of sperm from *t*/*t* animals have identified defective sperm flagellar function as the major physiological basis of *t*-specific male sterility (Olds-Clarke and Johnson 1993; Pilder et al. 1993, 1997; Redkar et al. 1998). In fact, a markedly discernible attribute of *t*/*t* male sterility is the sperm flagellar waveform defect, "curlicue" (Olds-Clarke and Johnson 1993), previously mapped to the largest and most distal inversion, *In[17]4*, coincident with the powerful *Tcd* /*Tcs2* factor (Fig. 1; Pilder et al. 1993). However, until recently, +/*t* recombination suppression had rendered the ability to investigate *t*-specific male traits at the molecular level a difficult task at best.

Of late, an indirect approach for high-resolution mapping of *t*-specific male sterility genes has been devised. Its usefulness has derived from the serendipitous finding that *Mus musculus domesticus* (*Domesticus*) males heterozygous for a *t* haplotype and an introgressed *Mus spretus* (*Spretus*) Chr 17 homolog (*S*) are sterile (Pilder et al. 1991). Because *S* and + Chr 17 homologs are not inverted relative to each other in inversions *In[17]1*, *In[17]3*, and *In[17]4* (the *t* complex regions housing the *Tcd/Tcs* factors; Hammer et al. 1989; Lyon 1984, 1986), intra-inversion *S*-+ recombinant Chr 17 homologs can and have been produced to genetically localize the *S*/*t* male sterility trait to high resolution via a combined fertility rescue/marker content mapping procedure (Pilder et al. 1991; Samant et al. 1999).

In terms of *t*-specific sperm flagellar defects mapping within the 10-cM *In[17]4*, a 1-cM *S*/*t* male sterility locus named *Hybrid Sterility 6* (*Hst6*) has proved provocative (Pilder et al. 1993). All males heterozygous for the *Spretus* allele of *Hst6* and a *t* haplotype ($Hst6^s$/*t*) are sterile. Moreover, sperm from $Hst6^s$/*t* males behave nearly identically to sperm from *t*/*t* males in exhibiting the "curlicue" flagellar waveform defect (Pilder et al. 1993). Interestingly,

Correspondence to: S.H. Pilder

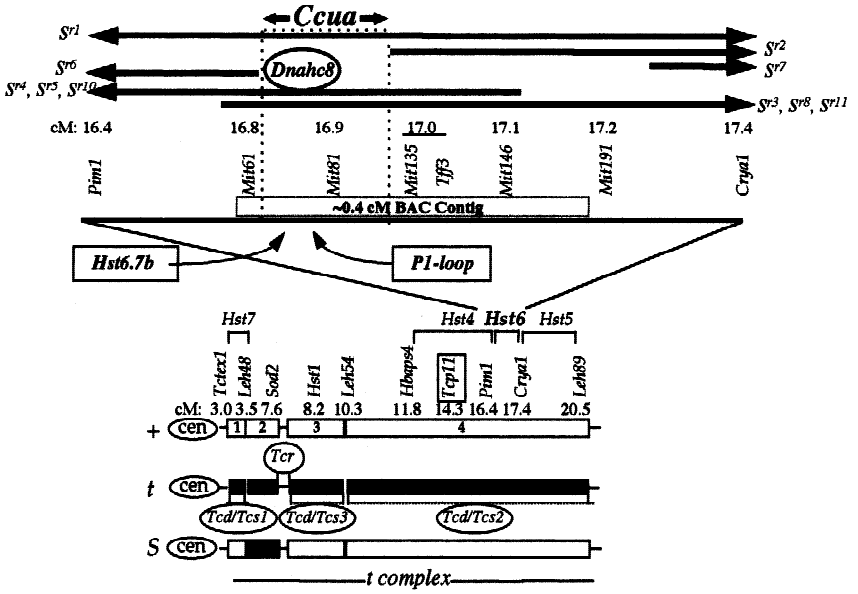

Fig. 1. Diagram of three *t* complex homologs (bottom) and enlargement of the *Hst6* locus (top). The three horizontal series of rectangles (bottom half of figure) represent the *Domesticus* wild-type (+) homolog (top), the *t* haplotype (*t*) homolog (middle), and the *Spretus* (*S*) homolog (bottom). The abbreviation for each homolog is to the left of its centromere, represented by the encircled abbreviation "cen". Boxes represent *t*-associated inversions, *In[17]1–In[17]4*, shown as 1, 2, 3, and 4 within the + homolog. Differences in color of the boxes (black vs. white) illustrate the orientation of each inversion in a homolog relative to its counterpart in other homologs. The positions of the *t*-specific male distorter/sterility factors, *Tcd/Tcs1*, *Tcd/Tcs2*, and *Tcd/Tcs3* and that of the *t* complex responder, Tcr, are shown below and above the *t* haplotype, respectively. Map positions of various markers are shown above the + homolog in wild-type orientation. The relative positions of *Hst4*, *5*, *6*, and *7* are shown above these markers. The 1-cM *Hst6* locus is shown enlarged (top) flanked by markers *Pim1* and *Crya1*. Map positions of various markers spanning *Hst6* are shown above the enlarged locus, as are the relative positions of the *Ccua–Tff3* BAC contig (long thin rectangle enclosing the words "~0.4 cM BAC Contig"), the *Curlicue a* locus (black arrows flanking the abbreviation "*Ccua*" with dotted lines extending below to the enlarged locus), and the position of *Dnahc8* in the *Ccua* locus (ellipse enclosing the abbreviation "*Dnahc8*"). The relative map positions within the BAC contig of *Hst6.7b* and the *P1-loop* region of *Dnahc8* are indicated by curved arrows from below the contig. Near the top of the diagram are six thin horizontal black rectangles representing the *Spretus* chromatin in ten *S*-+ recombinant homologs used to define the *Ccua* locus (Redkar et al. 1998; Samant et al. 1999). An arrowhead at an end(s) of a homolog signifies that its *Spretus* chromatin extends beyond the end(s) of the *Hst6* locus. S^{rx} recombinant Chr 17 homologs S^{r1}, S^{r2}, etc. have been previously described (Redkar et al. 1998; Samant et al. 1999).

all $Hst6^s$ homozygous males are also sterile; however, sperm produced by these males are completely immotile, owing to the inability to properly assemble a functional (or even recognizable) flagellum (Pilder et al. 1993; Phillips et al. 1993). This testis-specific flagellar development mutation (since named "whipless"; Samant et al. 1999) is first observed early in spermiogenesis as a defect in assembly or stabilization of the flagellar axonemal microtubules, resulting in sperm with ultrastructurally normal heads carrying caudally appended bags of cytoplasm containing disorganized flagellar elements (Phillips et al. 1993).

The *Hst6* allele-dependent expression of two different flagellar phenotypes implies that, in the *Domesticus* background, $Hst6^s$ behaves like a null or complete loss-of-function allele, totally recessive to $Hst6^t$, an altered-function mutation (Pilder et al. 1993). Thus, sperm from an $Hst6^s/Hst6^t$ compound heterozygous male would be, in effect, functionally hemizygous for $Hst6^t$ and, thus, phenotypically homozygous for $Hst6^t$. Additional studies have culminated in the high-resolution mapping of both "curlicue" and "whipless" to *Curlicue a* (*Ccua*), a < 0.2-cM sub-locus of *Hst6* (Fig. 1; Redkar et al. 1998; Samant et al. 1999).

In the present study, we describe the isolation of a cDNA fragment, *Hst6.7*, that maps to the proximal end of *Ccua* and recognizes an ~15-kb message expressed in the wild-type *Domesticus* testis, but not in the testis of "whipless" animals. We further report the cloning of the entire *Ccua* locus and present evidence that *Hst6.7* is the 3′-end of a testis specifically expressed gene, *Dnahc8* (Vaughan et al. 1996), encoding an axonemal dynein heavy chain. We also show that the mRNA expression characteristics displayed by *Dnahc8* are consistent with its having a species-specific fundamental role in sperm flagellar development and function, and furnish data that support the idea that the *t* allele of *Dnahc8* is a strong candidate for an essential component of the *t*-specific male sterility phenotype, *Tcd/Tcs2*. The potential ability of this gene and/or other testis-expressed members of multigene families to affect the evolution and maintenance of species barriers is discussed.

Materials and methods

Mice and genotyping. All recombinant lines of mice used in these experiments were bred and maintained in the colony of S.H. Pilder and carried either the C57BL/6, 129/Sv^{c+p+}, (C57BL/6 × 129/Sv^{c+p+}) F_1, or (129/Sv^{c+p+} × C57BL/6) F_1 genetic background. *Mus spretus* animals were originally obtained from M. Potter (Bethesda, Md.), and have been described (Hammer et al. 1989; Pilder et al. 1991). The breeding strategy used to produce test animals carrying various *S*-+ recombinant Chr 17 genotypes and the strategy for genotyping them have been described (Pilder et al. 1991, 1993; Pilder 1997; Redkar et al. 1998; Samant et al. 1999). In brief, recombinant Chr 17 homologs were defined by either PCR or Southern blot analysis according to the alleles present at the *In[17]4* marker loci: *D17Leh54*, *Hbaps4*, *Pim1*, *Crya1*, *D17Leh89* *D17Mit61*, *D17Mit81*, *D17Mit135*, *D17Mit146*, *D17Mit191* (Hamvas et al. 1998), the rat *P1-loop* ortholog of *Dnahc8*, *RK7-25* (Vaughan et al. 1996), and *Hst6.7* (as well as *Hst6.7b*, formerly referred to as a member of the *Spretus–Hst6p* sequences [Redkar et al. 1998] and *H6.7b* [Samant et al. 1999]). The Genbank Accession No. for the *Hst6.7* nucleotide sequence is AF117305. Oligonucleotide primer pairs for *D17Mit* markers were purchased from Research Genetics (Huntsville, Ala.).

BAC DNA isolation and analysis. BAC clones were identified and isolated from the CITB-CJ7 library (Research, Genetics) by PCR with oligonucleotide primers made from the sequences of overlapping BAC ends, and BAC DNAs were extracted and size-analyzed by inverse field gel electrophoresis as previously described (Samant et al. 1999). The >0.4-cM *Ccua-Tff3* contig consisted of the following nine contiguously overlapping BAC clones from proximal to distal: 99D17, *324M10*, 98H21, 351H18, *138O17*, *283H8*, *173G10*, *566K2*, 300K16. Underlined BACs have been previously described (Samant et al. 1999). Localization of *Hst6.7b* and the *Dnahc8 P1-loop* within the BAC contig was performed by hybridization of *Hst6.7b* and the *Dnahc8 P1-loop* to Southern blots of *TaqI* digests of all clones followed by comparison of hybridization patterns to *TaqI* digests of wild-type genomic DNA digests. Additional analysis of the position of *Hst6.7b* relative to the *Dnahc8 P1-loop* was performed by hybridization of T7 and SP6 BAC vector-end probes and *Hst6.7b* and the *Dnahc8 P1-loop* to Southern blots of *NotI-MluI* double digests of 98H21.

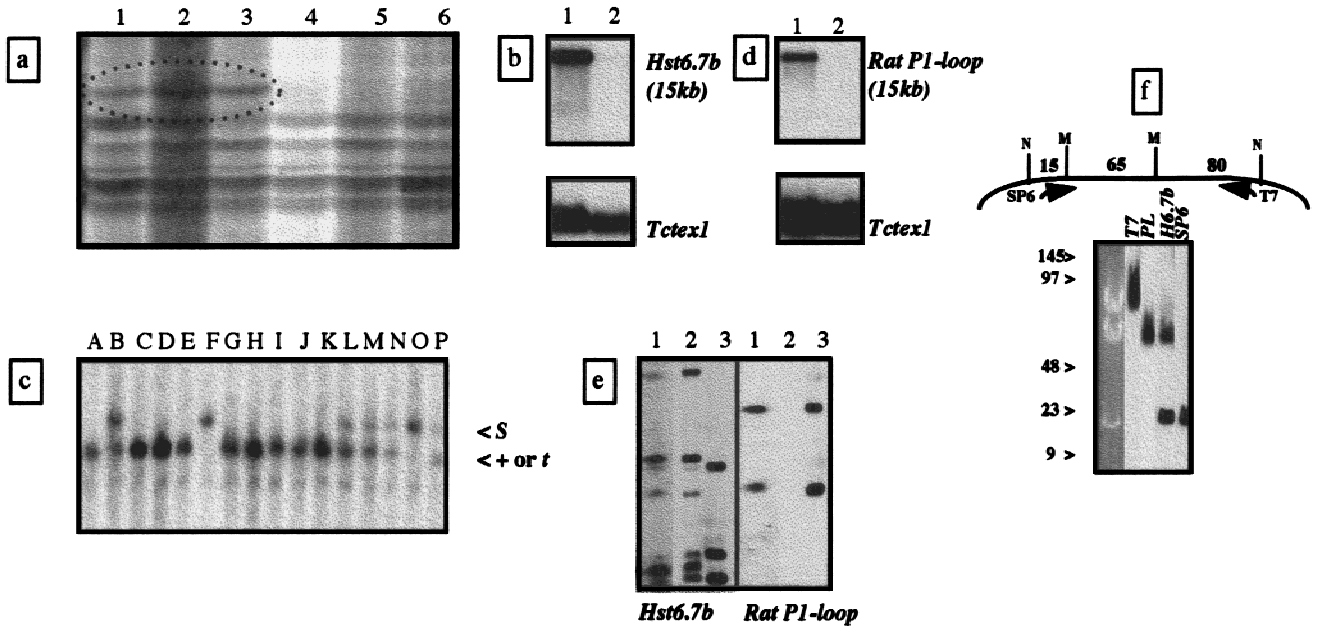

Fig. 2. Identification and linkage of *Dnahc8* to *Ccua*. **(a)** Differential display gel showing radiolabeled *Hst6.7* cDNA in lanes 1, 2, and 3 (from testis mRNA of wild-type control sibs), absent in lanes 4, 5, and 6 (from testis mRNA of *Ccua*^{s} homozygous sibs [line S^{r10} homozygotes]). **(b)** Northern analysis of mRNA from testis of wild-type control (lane 1) and S^{r10} homozygote (lane 2). *Hst6.7b* recognized an ~15-kb mRNA species in the control but not mutant lane. As a control for equal RNA loading, blot was stripped and reprobed with *Tctex1* cDNA (Hamvas et al. 1998), a dynein light chain gene mapping to the *Tcd/Tcs1* locus (see Fig. 1). **(c)** Southern blot analysis of *Sph*I-digested DNAs extracted from tail-tip biopsies of mice carrying *S*-+ recombinant Chr 17 homologs (Samant et al. 1999). [A] 129/Sv-+/+, [B] 129/Sv-*S*/+, [C] C57BL/6-+/+, [D] 129/Sv-+/t^{w5}, [E] C57BL/6-+/t^{w32}, [F] 129/Sv-S^{r1}/S^{r1}, [G] (129/SvXC57BL/6)F1-t^{w32}/t^{w5}, [H] 129/Sv-S^{r2}/S^{r2}, [I] C57BL/6-S^{r7}/S^{r7}, [J] (129/SvXC57BL/6) F1-S^{r6}/t^{w32}, [K] 129/Sv-S^{r6}/S^{r6}, [L] 129/Sv-S^{r3}/t^{w5}, [M] (129/SvXC57BL/6)F_1-S^{r4}/t^{w32}, [N] 129/Sv-S^{r5}/t^{w5}, [O] C57BL/6-S^{r10}/S^{r10}, [P] (129/SvXC57BL/6)F_1-S^{r8}/t^{w32}. **(d)** Northern blot of same samples as in (b) probed with rat *Dnahc8 P1-loop* ortholog (Vaughan et al. 1996) and *Tctex1*. **(e)** Southern blot of *Taq*I -digested 129/Sv-+/+ genomic DNA (1) and BACs 324M10 (2) and 98H21 (3), probed with *Hst6.7b* (left), then stripped and reprobed with the *Dnahc8 P1-loop* (right). **(f)** At the top, a diagram of the BAC clone, 98H21. N = *Not*I; M = *Mlu*I; *T7* and *SP6* followed by arrows = the *T7* and *SP6* promoter regions of the BAC vector, respectively, with arrows pointing in from the ends of the mouse DNA insert. The numbers 15, 65, and 80 represent the sizes in kb of the fragments of the *Not*I-*Mlu*I digest of the insert. Below, the diagram is a Southern blot of this digest. To the left are size markers in kb. Left-hand lane is a photograph of the digest of the insert, with four right-hand lanes representing patterns of hybridization of four probes (identified above each lane) to that digest.

Differential display-PCR. Differential display-PCR was performed as previously described (Liang and Pardee 1992) with the following modifications. Primer pair sequences were identical to those in the RNAimage Kit (GenHunter Corporation, Nashville, Tenn.) including all three one-base anchored oligo-dT primers (16mers) and 65 to 80 arbitrary 13mers (detecting approximately 93% of mRNAs) in the total population. The primer pair used to detect *Hst6.7* was 5′-AAGCT$_{11}$G-3′ and 5′-AAGCTT-CCTCTAT-3′. RNA samples from the testes of three mutant and three congenic control sibs were isolated and independently subjected to Reverse Transcription-PCR (RT-PCR). Poly-A+ rather than total RNA samples were used in each reaction. cDNA products were loaded in six adjacent lanes of a differential display gel (Fig. 2a). Only radiolabeled bands visualized in all three control lanes but in no mutant lane (or vice versa) were selected for further analysis. DNA samples isolated from gel slices were cloned, DNA was extracted from 12 single colony isolates of each cloning experiment, and each extracted DNA sample was subjected to DNA fingerprint analysis, with four cutter restriction enzyme digests separated on 3% Metaphor agarose gels (FMC, Rockville, Me.)

RNA isolation and Northern blot analysis. RNA samples were extracted from various tissues, followed by treatment with RNase-free DNase (Promega, Madison, Wis.) for 30 min at 37°C, and in some cases by oligo-dT selection for poly-A+ mRNA. Equal aliquots of RNA were loaded on 1.0% agarose-formaldehyde gels and electrophoresed at 125V until the Xylene Cyanol dye front had migrated 2/3 the length of the gel. Gels were photographed, then blotted to positively charged nylon membranes, and membranes were hybridized with α-^{32}P radiolabeled probes. Molecular weight markers were purchased from Life Technologies (Gaithersburg, Md.). After stripping and before reprobing blots, the remaining label was allowed to decay until no longer visible upon overnight exposure of blots to film.

Results

Identification of a Hybrid Sterility 6 gene candidate. In order to identify the gene responsible for presentation of *Hst6*-specific flagellar phenotypes, we took advantage of the assumption that the *Spretus* allele of the *Hst6*-specific sub-locus, *Ccua* (*Ccua*^{s}), behaved like a null allele in the *Domesticus* testis (Pilder et al. 1993; Phillips et al. 1993; Samant et al. 1999). We reasoned that absent or reduced *Ccua*^{s} mRNA expression in the testis might be the basis for the homozygous *Ccua*^{s} null phenotype (“whipless”). Therefore, we employed differential display-PCR (Liang and Pardee 1992) of mRNAs extracted from the testes of the S^{r10} (Fig. 1) line of *Ccua*^{s}/*Ccua*^{s} (sterile mutant) animals and +/+ fertile congenic controls in an attempt to isolate the 3′ ends of mRNA species expressed in control but not mutant testes. Only one gel band, hereafter referred to as *Hst6.7*, exhibited clear differential display between wild-type control and mutant samples (Fig. 2a). With purified *Hst6.7* DNA as a probe, a larger (~2 kb) cDNA fragment (called *Hst6.7b*) was isolated from a 129/Sv^{c+p+} testis cDNA library (Pilder et al. 1992). Sequence analysis showed that *Hst6.7b* contained *Hst6.7* (data not shown).

Interestingly, several differential display gel artifacts were observed that apparently evolved from *Spretus–Domesticus* nucleotide sequence differences, giving rise to small (usually one to several nucleotides) control versus mutant gel band shifts. Purification and subsequent sequence analysis of several of these "differentially displayed" (but not differentially expressed) DNA species identified all of them as exon fragments of *Tcp11* (data not shown), a gene mapping proximal to *Hst6* (and thus *Ccua*) by more than 2 cM on the Chr 17 map (Mazarakis et al. 1991; Hamvas et al. 1998), but present in the proximal extent of *Spretus* chromatin in the genome of the mutant line of mice used in the differential display experiment. However, *Tcp11* could be ruled out as a candidate gene for "whipless" and/or "curlicue" for four reasons: (1) it mapped proximal to both *Ccua* and *Hst6;* (2) control and mutant *Tcp11* alleles were not differentially expressed (data not shown); (3) other "whipless"/"curlicue" mutant lines of mice did not carry the *Spretus* allele of *Tcp11* (Redkar et al. 1998; Samant et al. 1999); and (4) all *In[17]4 S-+* recombinant Chr 17 lines of mice heterozygous for a *t* haplotype and $Tcp11^{s}Ccua^{+}$ or homozygous for $Tcp11^{s}Ccua^{+}$ were fertile and produced sperm exhibiting neither the "curlicue" nor "whipless" phenotype, respectively (Redkar et al. 1998; Samant et al. 1999).

Because *Hst6.7* was the only clearly differentially displayed band identified, *Hst6.7b* was subsequently employed to probe a Northern blot containing the mRNA samples used in the differential display experiments. A highly expressed mRNA of ~15 kb was detected in the control sample; however, no signal was evident in the mutant mRNA sample (Fig. 2b). Southern blot-RFLP analysis demonstrated that *Hst6.7b* mapped to the <0.2-cM *Ccua* locus (Fig. 1; Redkar et al. 1998; Samant et al. 1999).

The large size (~15 kb) of the mRNA species recognized by *Hst6.7b,* and the medium-resolution mapping of an axonemal dynein heavy chain gene, *Dnahc8* (Vaughan et al. 1996), to a location in the vicinity of *Ccua* in the mouse (whose rat ortholog appeared by Northern analysis to be testis specifically expressed; Tanaka et al. 1995), led us to speculate that *Hst6.7b* might represent part of *Dnahc8.* However, very little of the sequence of *Dnahc8* was known, and the sequences of *Hst6.7* and *Hst6.7b* showed no significant similarity to any sequence in Genbank (data not shown). Thus, we performed high-resolution mapping (Samant et al. 1999) of *Dnahc8* to determine its precise position relative to *Ccua.* A Southern blot of restriction enzyme digested DNAs extracted from lines of mice carrying various combinations of *S-+* recombinant Chr 17 homologs, including a subset carrying the $Ccua^{s}$ allele either heterozygously or homozygously (Figs. 1 & 2c; Redkar et al. 1998; Samant et al. 1999) was probed with a rat sequence (*RK7-25*) orthologous to the highly conserved *P1-loop* region (the ATP binding domain) of *Dnahc8* (Vaughan et al. 1996). The *Dnahc8*-specific *P1-loop* co-localized with *Hst6.7b* at the *Ccua* locus, suggesting that *Hst6.7b* and the *Dnahc8* rat *P1-loop* sequence were different ESTs from orthologs of the same gene. Probing a Northern blot identical to the one shown in Fig. 2b with the rat *Dnahc8 P1-loop* sequence produced the same results as those observed when *Hst6.7b* was used as probe (Fig. 2d), reinforcing the idea that *Hst6.7b* was part of *Dnahc8.*

Physical association of Hst6.7b and Dnahc8 P1-loop with Ccua. We further examined the genetic organization of *Hst6.7b* and *Dnahc8 P1-loop* with respect to *Ccua* and each other by extending two small BAC (bacterial artificial chromosome) contigs (the *Ccua* and the *Tff3* [Trefoil Factor 3] contigs; Samant et al. 1999) both proximally and distally to produce a single larger contig of nine BACs (see Materials and methods) covering the region from approximately 16.775 cM to approximately 17.175 cM on the Chr 17 map (Fig. 1; Hamvas et al. 1998). We screened Southern blots containing *Taq*I restriction endonuclease digests of all BAC clones in this contig with two probes, *Hst6.7b* and the rat *Dnahc8 P1-loop* ortholog. *Hst6.7b* hybridized to the digest of the second-most proximal BAC (324M10), producing the hybridization pattern identical to that seen when *Hst6.7b* was hybridized to the same digest of genomic DNA from a control animal (Fig. 2e; Samant et al. 1999). *Hst6.7b* also hybridized to a subset of the same bands on the next more distal BAC (third-most proximal BAC in the contig, 98H21). The *P1-loop* probe hybridized only to 98H21, the third-most proximal BAC in the contig, producing a hybridization pattern identical to one seen on Southern blots of genomic DNA from a control animal (Figs. 1 & 2e). These results suggested that *Hst6.7b* and the *Dnahc8 P1-loop* might represent sequences from the same gene.

In order to orient the *Dnahc8 P1-loop* and *Hst6.7b* with respect to each other, we performed BAC end sequence analysis of 324M10 and 98H21. This analysis demonstrated that 324M10 and 98H21 mouse DNA inserts overlapped at the ends of each adjacent to the vector's *SP6* promoter region (data not shown). We then digested the 98H21 BAC clone with *Not*I and *Mlu*I, followed by separation of the products of this digest on a 1.0% agarose inverse field gel (Fig. 2f). Digestion with *Not*I essentially separated the vector from the mouse DNA insert of the BAC clone, with minimal vector sequences left attached to the ends of the insert containing the *T7* promoter on one end (the distal end in this case), and the *SP6* promoter on the other end (the proximal end in this case). Digestion with *Mlu*I cut the mouse insert released from the vector by *Not*I into several smaller pieces (~80 kb, ~65kb, and ~15 kb; Fig. 2f). A Southern blot of this digest was hybridized sequentially to four different probes: one made from the *T7* end of the BAC vector, one from the *SP6* end of the vector, *Hst6.7b,* and the *Dnahc8 P1-loop.* The *SP6* probe hybridized to the ~15-kb fragment, while the *T7* probe hybridized to the ~80-kb fragment, demonstrating that the ~15-kb fragment was the proximal fragment of the mouse insert, the ~65-kb fragment was the central fragment, and the ~80-kb fragment was the distal fragment of the mouse insert (Fig. 2f). As expected, *Hst6.7b* hybridized to the ~15-kb fragment, but it also hybridized to the 65-kb central fragment (Fig. 2f). The *Dnahc8 P1-loop* hybridized exclusively to the 65-kb central fragment (Fig. 2f). These data demonstrated that the distance between the distal end of *Hst6.7b* and the *Dnahc8 P1-loop* was no more than 65 kb in the genome.

In addition, we were able to extend the *Hst6.7b* cDNA clone only at one end (the end opposite its oligoadenylated end; data not shown) when it was used to isolate overlapping clones from a random-primed mouse testis cDNA library, suggesting that *Hst6.7b* was the 3′-end of a message. The fact that the 3′-end of an axonemal dynein heavy chain mRNA is ~10 kb away from the *P1-loop* region, together with our finding that *Hst6.7b* is a maximum of 65 kb from the *Dnahc8 P1-loop* in the genome strongly suggested that *Hst6.7b* was the 3′-end of *Dnahc8.*

Dnahc8 mRNA expression in the testis commences just prior to the onset of sperm flagellar development. The stages of developing germ cells present at various times post-partum in the adolescent mouse testis have previously been resolved by flow cytometry (Malkov et al. 1998). Thus, we determined the onset of *Dnahc8* RNA expression in the *Domesticus* testis by probing Northern blots of total RNA extracted from the testes of 7, 10, 14, 18, and 21 days post-partum (pp), and from 10-week-old (adult) wild-type mice with the *Dnahc8 P1-loop* (Fig. 3a, top). *Dnahc8* RNA expression was first evident in late pachytene (18 days pp), and began to increase in early spermiogenesis (21 days pp). Thus, the appearance of *Dnahc8* mRNA expression occurred just prior to the onset of sperm tail development (Fig. 3a; Oko and Clermont 1990). When the same blot was reprobed with *Hst6.7b,* the identical result ensued (Fig. 3a, middle), suggesting once again that *Hst6.7b* and the *Dnahc8 P1-loop* were fragments of the same gene.

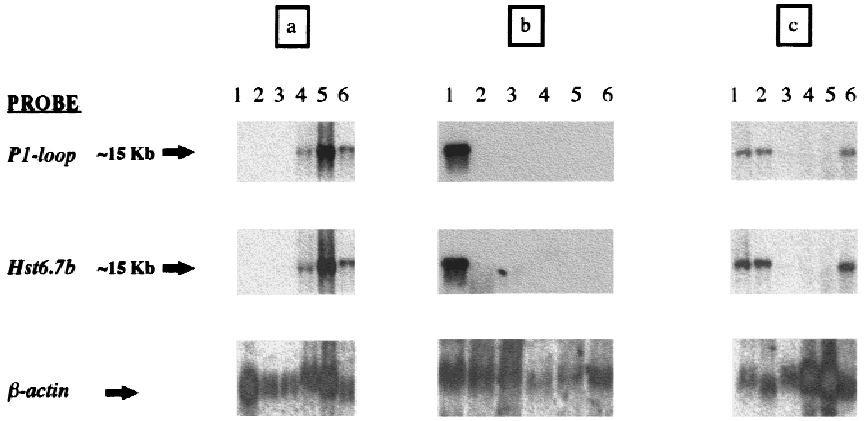

Fig. 3. *Dnahc8* mRNA expression characterized by Northern blot analysis. **(a)** Expression in the adolescent and adult testis. Stages of seminiferous epithelial development in the mouse have been determined previously by flow cytometry (Malkov et al. 1998). [1] 7-day post-partum (spermatogonia only), [2] 10-day post-partum (spermatogonia to leptotene spermatocytes), [3] 14-day post-partum (spermatogonia to early pachytene spermatocytes), [4] 18-day post-partum (spermatogonia to late pachytene spermatocytes), [5] 21-day post-partum (spermatogonia to round spermatids), [6] 10-week (adult; spermatogonia to testicular spermatozoa). Blot was probed with the *Dnahc8 P1-loop* (top) and, after stripping, with *Hst6.7b* (middle). **(b)** Expression in multiple male mouse tissues. [1] testis, [2] lung, [3] heart, [4] kidney, [5] liver, [6] brain. Blot was probed with the *Dnahc8 P1-loop* (top) and, after stripping, with *Hst6.7b* (middle). **(c)** Expression in the adult testis of [1] C57BL/6-+/+, [2] 129/Sv-S^{r2}/S^{r2}, [3] 129/Sv-S^{r11}/S^{r11}, [4] (129/SvXC57BL/6)F_1-S^{r3}/S^{r3}, [5] *M. spretus*, [6] (129/SvXC57BL/6)F_1-t^{w5}/t^{w32}. Probes for *Dnahc8* expression were the *Dnahc8 P1-loop* (top) and *Hst6.7b* (middle). Control for RNA loading in parts a, b, and c was human β-actin cDNA (bottom).

Dnahc8 mRNA expression is testis-specific in the Mus musculus domesticus adult male, but not in Mus spretus. A *Domesticus* adult male multi-tissue Northern blot probed with the *Dnahc8 P1-loop* indicated that *Dnahc8* was testis specifically expressed, at least at the resolution of Northern analysis (Fig. 3b, top). Once again, the identical result was obtained when the blot was reprobed with *Hst6.7b* (Fig. 3b, middle).

However, when adult testis mRNAs, extracted from *Domesticus* control mice, three lines of mice homozygous for various *Spretus-Domesticus* recombinant Chr 17 homologs (see Fig. 3c legend & Fig. 1), *Spretus* mice, and *t/t* mice, were examined for expression of *Dnahc8* on Northern blots probed with either the rat *Dnahc8 P1-loop* ortholog (Fig. 3c, top) or with *Hst6.7b* (Fig. 3c, middle), expression was not evident in the testes of any of the $Ccua^s/Ccua^s$ lines or, to our surprise, in the *Spretus* testis. After long exposures of blots to film (several days), faint ~15-kb bands could be seen in $Ccua^s/Ccua^s$ and *Spretus* lanes, implying either that *Dnahc8* is expressed at a very basal level in the *Spretus* testis and the testis of "whipless" animals, or that our probes weakly cross-hybridized with mRNAs of other members of the large dynein heavy chain gene family (data not shown). In either event, the testis-specific nature of *Dnahc8* expression in *Domesticus* and the striking difference between *Dnahc8* expression in the *Domesticus* and *Spretus* testes indicated that the regulation of *Dnahc8* expression in these two *Mus* species had recently diverged.

Discussion

Is Hst6.7b a cDNA fragment of Dnahc8? Significant nucleotide sequence data pertaining to mammalian axonemal dyneins are not available. Since the *Dnahc8* transcript is very large as well as a member of a sizable, highly conserved multigene family (Tanaka et al. 1995; Vaughan et al. 1996), the ability to isolate a full-length, non-chimeric *Dnahc8* cDNA and thus, link *Hst6.7b* to the *Dnahc8 P1-loop* definitively is a difficult process, requiring the sequencing of a genomic BAC clone (98H21) in its entirety. However, we have demonstrated here that both *Hst6.7b* and the *Dnahc8 P1-loop* map to the <0.2-cM *Ccua* locus, and that part of *Hst6.7b* and all of the *P1-loop* map to the same ~65-kb *Mlu*I fragment of the 98H21 BAC clone (Figs. 1 & 2f). Furthermore, by using *Hst6.7b* to probe a random-primed mouse testis cDNA library, we have been able to extend *Hst6.7b* only at the end opposite its oligoadenylated end, suggesting that *Hst6.7b* is the 3′-end of a message. Its proximity to the *Dnahc8 P1-loop* region in the genome implies that *Hst6.7b* is the 3′-end of *Dnahc8*, with the direction of transcription being telomeric to centromeric on Chr 17.

In addition, both *Hst6.7b* and the *Dnahc8 P1-loop* recognize ~15-kb transcripts in wild-type but not "whipless" or *Spretus* testis mRNA samples (Figs. 2b, 2d, 3c). Furthermore, the testicular temporal expression attributes and tissue specificity of *Dnahc8* transcription appear to be identical to those characteristics of *Hst6.7b* expression (Fig. 3a,b). These data, together with the previous mapping of only one dynein heavy chain gene, *Dnahc8*, to mouse Chr 17 (Vaughan et al. 1996) strongly suggest that *Hst6.7b* is part of *Dnahc8.*

An evaluation of the hypothesis that male-specific t haplotype-mediated phenotypes result from the expression of defective dyneins. On the basis of numerous physiological and genetic studies of sperm from +/*t* and *t/t* animals (see Olds-Clarke 1997, for a recent review), a "defective dynein" model has been described in which the combined expression of *t* alleles of several genes encoding components of axonemal dyneins would serve as the molecular basis for *t* -specific male traits (Harrison et al. 1998). While this theoretical model is supported indirectly by the logical linkage of numerous (and diverse) findings, major support derives from the fact that two testis-expressed dynein light chain genes, *Tctex1* and *Tctex2*, co-localize with the *Tcd/Tcs1* and *Tcd/Tcs3* loci, respectively (each encodes an alternative + and *t* form in mice, each is a component of an axonemal dynein in *Chlamydomonas*, and each is found in +- and *t*-bearing mouse sperm; Harrison et al. 1998; Patel-King et al. 1997; Huw et al. 1995; Lyon 1984, 1986). The model goes on to suggest that in +/*t* heterozygotes, the testis would produce +-bearing gametes carrying mostly defective *t* dyneins in their axonemes, and *t*-bearing gametes carrying mostly + dyneins in theirs, owing to a dynamic competition between allelic "gatekeepers", Tcr^+ and Tcr^t, for the anchorage of wild-type dynein components into the axonemes of *t*-bearing or +-bearing sperm (Patel-King et al. 1997). Of course, in *t/t* homozygotes, the nature of *Tcr* alleles would be irrelevant, because only defective *t* dynein components would be available for assembly into sperm tails. Thus, all *t/t* males would be sterile because their sperm would be unable to reach the site of fertilization and/or penetrate the egg investments owing to severe dynein dysfunction.

The present study provides additional circumstantial support for the "defective dynein" model by supplying a molecular candidate, a gene encoding an axonemal dynein heavy chain (*Dnahc8*), for the most powerful of the *t* distorter/sterility elements, *Tcd/Tcs2*. The high-resolution genetic association of *Dnahc8* with "curlicue", and the timing and nature of *Dnahc8* mRNA expression in *Domesticus* males (Fig. 3a,b; Lyon 1984, 1986; Papaioannou et al. 1979; Seitz and Bennett 1985; Oko and Clermont 1990) lends

credence to this candidacy. In addition, the absence of *Dnahc8*^{s} expression in the testis of the *Dnahc8*^{s}/*Dnahc8*^{s} homozygote unmasks the deleterious consequences of *Dnahc8*^{t} on flagellar motility and male fertility in both the *Dnahc8*^{s}/*Dnahc8*^{t} heterozygote and the *Dnahc8*^{t}/*Dnahc8*^{t} homozygote, and reinforces the idea that *Dnahc8*$^{+}$ expression is required for +/*t* male fertility. However, the effect of *Dnahc8* on meiotic drive remains unclear. Furthermore, whether *Dnahc8*^{t} expression is sufficient, in the absence of expression of the *t* alleles of other nearby sperm function genes (Pilder et al. 1991, 1993; Redkar et al. 1998; Samant et al. 1999), to generate the full range and power of *Tcd/Tcs2* effects is, at best, equivocal. Nonetheless, the isolation of a strong candidate, *Dnahc8*, for *Tcd/Tcs2* will allow us to perform direct tests of the "defective dynein" model to determine the sufficiency and/or necessity of *Dnahc8*^{t} expression for the presentation of the full range of male-specific *t* haplotype-mediated effects.

Implications of Dnahc8 bifunctionality. A correlation between the expression of a defective axonemal dynein heavy chain allele (*Dnahc8*^{t}) and the observation of an abnormal flagellar waveform phenotype ("curlicue") is not unexpected, since propagating a coherent flagellar beat depends on synchronously coordinating the activities of multiple, genetically independent axonemal dynein heavy chain isoforms (Brokaw and Kamiya 1987; Witman 1992; Holzbaur and Vallee 1994; Asai and Lee 1995; Asai 1995; Vallee and Sheetz 1996). To date, however, no role in the assembly or stable maintenance of the developing flagellum has been described for axonemal dyneins. In *Chlamydomonas*, loss-of-function mutations in either KINESIN II or the cytoplasmic dynein heavy chain DHC1b (known as DHC2 in mammals) have been shown to result in cells that either lack flagella or have short, dysfunctional flagella (Cole et al. 1998; Pazour et al. 1998, 1999; Porter et al. 1999). Thus, both KINESIN II and the cytoplasmic dynein DHC1b are thought to be the major tubulin-based molecular motors driving the anterograde and retrograde movements, respectively, of the flagellar assembly mechanism known as intraflagellar transport (IFT; Bloch and Johnson 1995; Johnson 1995; Cole et al. 1998; Pazour et al. 1998, 1999; Porter et al. 1999; Rosenbaum et al. 1999). However, the unexpected connection between a phenotype of aberrantly assembled sperm tails ("whipless") and the absence of expression of an axonemal dynein heavy chain gene (*Dnahc8*) in the testis of experimental animals argues for a more dynamic interpretation of dynein heavy chain form and function in the flagellar assembly process, especially in complex multicellular organisms (Witman 1992; Holzbaur and Vallee 1994; Asai 1995; Dutcher 1995; Porter 1996; Rosenbaum et al. 1999).

The mammalian spermatozoon has developed numerous adaptations to cope with the multiple obstacles it encounters in the lengthy female genital tract while in competition with millions of other sperm for the opportunity to fertilize very few eggs. Among these adaptations is a relatively long (especially in rodents), structurally complex, and highly differentiated tail that can respond to diverse signals in the female genital tract with extensive and rapid alterations in flagellar waveform properties. The putative bifunctionality of *Dnahc8* activity suggests that natural selection may have favored the recent evolution of mechanisms to cope with this increased intricacy of flagellar organization and function without increasing gene number: hence, dynein isoforms with both flagellar assembly ("cytoplasmic") and flagellar motility ("axonemal") functions. This viewpoint is supported not only by our findings concerning *Dnahc8*-related phenotypes, but, by studies of other mammalian cell types suggesting that multifunctional isoforms of dynein heavy chain as well as heavy chain genes whose transcripts undergo alternative splicing have developed in response to particular cellular demands (Vaisberg et al. 1994; Tanaka et al. 1995; Supp et al. 1997). Thus, the functional sorting of dyneins into "axonemal" and "cytoplasmic" classes so often used to describe

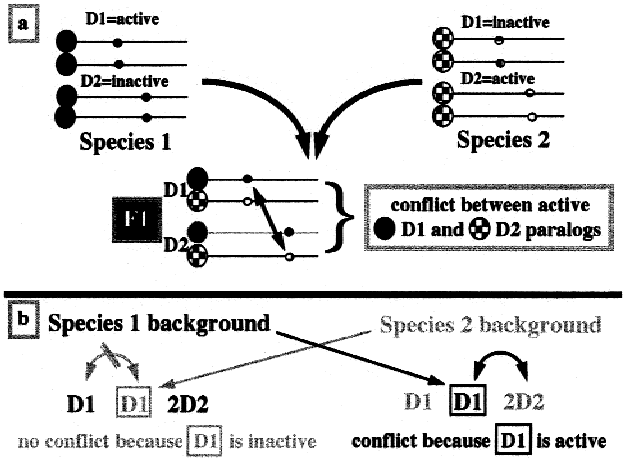

Fig. 4. (a) Hypothetical model of reproductive isolation caused by the expression of conflicting interspecific paralogs of a multigene family in the testis of the F_1 hybrid. Species 1 carries two copies of a gene (D1) active in the testis on one chromosome and two copies of an inactive paralog (D2) on a second chromosome. However, in Species 2, D1 is inactive in the testis and its paralog, D2, is active. An F_1 hybrid expresses both active paralogs in its testis, and non-coadapted (conflicting) gene products are shared by all developing spermatids via cytoplasmic bridges maintained between all meiotic partners. **(b)** Hypothetical model of asymmetric male sterility via reciprocal introgression of orthologs of a multigene family. On the left, the inactive ortholog D1 (boxed) from Species 2 is fully introgressed into the Species 1 background, where the D1 ortholog from Species 1 is actively expressed in the testis, while the D2 paralog from Species 1 is inactive. In this D1-Species 1/D1-Species 2 heterozygote, there is no conflict between orthologs (or paralogs) because of the nullipotency of the introgressed (inactive) D1 allele. On the right, the active ortholog D1 (boxed) from Species 1 is fully introgressed into the Species 2 background, where the D1 ortholog from Species 2 is inactive, but the D2 paralog from Species 2 is active in the testis. In this D1-Species 2/D1-Species 1 heterozygote, introgression of the Species 1 active D1 ortholog (boxed) into the Species 2 background produces a conflict between actively expressed, non-coadapted paralogs (D1 from Species 1 and D2 from Species 2 as seen in the F_1 hybrid in 4a).

heavy chain family members in organisms with simple flagella (Johnson 1995; Gibbons 1995; Tanaka et al. 1995) may no longer be entirely appropriate in more complex organisms.

Although no ortholog of *Dnahc8* has yet been mapped in the human genome (Vaughan et al. 1996), our findings demonstrate that mouse loci tightly linked to the *Dnahc8* locus map to human Chr 6p21.3 and to Chr 21q22.3. While no dynein heavy chain gene has yet been mapped to human Chr 21, an axonemal dynein heavy chain, *Dnahc6* (DLP6), located on mouse Chr 6 between closely linked markers that show conserved synteny with human Chr 2p12, has a human ortholog at Chr 6p21.3 (Vaughan et al. 1996). Thus, it is tempting to speculate that a recent expansion of dynein heavy chain function in relatively complex organisms might have resulted from recombinatorial processes such as gene conversion or exon shuffling between functional subunits of paralogous family members. Because the functional classification of dynein heavy chain isoforms in mammals has been based, to a large degree, on comparative phylogenetic analyses of their P1-loop nucleotide sequences (Gibbons 1995; Tanaka et al. 1995), it will be of considerable interest in the future to analyze other regions of mouse *Dnahc8* sequence, and to compare more extensively the sequences from *Dnahc8* with those from *Dnahc6* in the mouse and to the putative human ortholog of *Dnahc6*.

The testis specificity of *Dnahc8* expression in the rat and in *Mus musculus domesticus*, but not in *Mus spretus*, indicates that *Spretus* has lost the ability to express its *Dnahc8* allele in the testis within the relatively short time period in which the two mouse species have diverged (Silver 1995). However, *Spretus* must have

an alternative mechanism(s) for performing the functions assigned to *Dnahc8* in the *Domesticus* testis and sperm flagellum. If we assume that the role of *Dnahc8* in the *Spretus* testis is carried out by a paralogous member or members of the dynein heavy chain family, then we can postulate that the alternative expression of paralogous axonemal dynein heavy chain isoforms in the structurally elaborate sperm tails of closely related mammalian species, such as *Domesticus* and *Spretus*, reflects the rapid evolution of male fertility-related traits that contribute to the establishment and maintenance of species barriers (Fig. 4a; Maeda and Smithies 1986; Wu and Davis 1993; Wu and Palopoli 1994; Ting et al. 1998; Nurminsky et al. 1999). Indeed, the alternative expression of paralogous rather than orthologous dyneins (or paralogous members of other multigene families) in the testes of closely related species could, in part, account for the high frequency of asymmetric male sterility observed in the reciprocal introgression of orthologs between such species (Fig. 4b; Pilder et al. 1991; Ting et al. 1998). In the future, we will test this hypothesis by thoroughly dissecting the regulation of *Dnahc8* expression and the molecular basis of *Dnahc8* function in the mouse.

Acknowledgments. This study was supported by U.S. Public Health Service grant HD31164 to S.H. Pilder.

References

Asai DJ (1995) Multi-dynein hypothesis. Cell Motil Cytoskeleton 32, 129–132

Asai DJ, Lee SW (1995) The structure and function of dynein heavy chains. Mol Cells 5, 299–305

Bloch MA, Johnson KA (1995) Identification of a molecular chaperone in the eukaryotic flagellum and its localization to the site of microtubule assembly. J Cell Sci 108, 3541–3545

Brokaw C, Kamiya R (1987) Bending patterns of *Chlamydomonas* flagella. IV. Mutants with defects in inner and outer dynein arms indicate differences in dynein arm function. Cell Motil Cytoskeleton 8, 68–75

Cole DG, Diener DR, Himelblau AL, Beech PL, Fuster JC et al. (1998) *Chlamydomonas* kinesin-II-dependent intraflagellar transport (IFT): IFT particles contain proteins required for ciliary assembly in *Caenorhabditis elegans* sensory neurons. J Cell Biol 141, 993–1008

Dutcher SK (1995) Flagellar assembly in two hundred and fifty easy to follow steps. Trends Genet 11, 398–404

Gibbons IR (1995) Dynein family of motor proteins: present status and future questions. Cell Motil Cytoskeleton 32, 136–144

Hammer MF, Schimenti J, Silver LM (1989) Evolution of mouse Chromosome 17 and the origin of inversions associated with *t* haplotypes. Proc Natl Acad Sci USA 86, 3261–3265

Hamvas RMJ, Trachtulec Z, Vernet C, Forejt J (1998) Mouse Chromosome 17. Mamm Genome 8 (Suppl.) S320–S334

Harrison A, Olds-Clarke P, King SM (1998) Identification of the *t* complex-encoded cytoplasmic dynein light chain *Tctex1* in inner arm I1 supports the involvement of flagellar dyneins in meiotic drive. J Cell Biol 140, 1137–1147

Holzbaur ELF, Vallee RB (1994) Dyneins: molecular structure and cellular function. Annu Rev Cell Biol 10, 339–372

Huw L-I, Goldsborough AS, Willison K, Artzt K (1995) *Tctex2:* a sperm tail surface protein mapping to the *t* complex. Dev Biol 170, 183–194

Johnson KA (1995) Keeping the beat: form meets function in the *Chlamydomonas* flagellum. BioEssays 10, 847–854

Johnson LR, Pilder SH, Bailey JL, Olds-Clarke P (1995a) Sperm from mice carrying one or two *t* haplotypes are deficient in investment and oocyte penetration. Dev Biol 168, 138–149

Johnson LR, Pilder SH, Olds-Clarke P (1995b) The cellular basis for interaction of sterility factors in the mouse *t* haplotype. Genet Res 66, 189–193

Liang P, Pardee AB (1992) Differential display of eukaryotic messenger RNA by means of the polymerase chain reaction. Science 257, 967–971

Lyon MF (1984) Transmission ratio distortion in mouse *t* haplotypes is due to multiple distorter genes acting on a responder locus. Cell 37, 621–628

Lyon MF (1986) Male sterility of the mouse *t* complex is due to homozygosity of the distorter genes. Cell 44, 357–363

Maeda N, Smithies O (1986) The evolution of multigene families: human haptoglobin genes. Annu Rev Genet 20, 81–108

Malkov M, Fisher Y, Don J (1998) Developmental schedule of the postnatal rat testis determined by flow cytometry. Biol Reprod 59, 84–92

Mazarakis ND, Nelki D, Lyon MF, Ruddy S, Evans EP et al. (1991) Regulation and characterization of a testis-expressed developmentally regulated gene from the distal inversion of the mouse *t*-complex. Development 111, 561–571

Mcgrath J, Hillman N (1980) Sterility in mutant (t^{Lx}/t^{Ly}) male mice. III. In vitro fertilization. J Embryol Exp Morphol 59, 49–58

Nurminsky DI, Nurminskaya MV, Aguiar DD, Hartl DL (1999) Selective sweep of a newly evolved sperm-specific gene in Drosophila. Nature 10, 572–575

Oko R, Clermont Y (1990) Mammalian spermatozoa: structure and assembly of the tail. In *Controls of Sperm Motility: Biological and Clinical Basis*, C Gagnon, ed. (New York: CRC Press), pp 3–27

Olds-Clarke P (1997) Models for male infertility: the *t* haplotypes. Rev Reprod 2, 157–164

Olds-Clarke P, Johnson LR (1993) *t* Haplotypes in the mouse compromise sperm flagellar function. Dev Biol 155, 14–25

Papaioannou VE, Artzt K, Dooher GB, Bennett D (1979) Effects of chimaerism for two *T/t* complex mutations on sperm function. Gamete Res. 2, 147–151

Patel-King RS, Benashski SE, Harrison A, King SM (1997) A *Chlamydomonas* homolog of the putative murine *t* complex distorter *Tctex2* is an outer arm dynein light chain. J Cell Biol 137, 1081–1090

Pazour GJ, Wilkerson CG, Witman GB (1998) A dynein light chain is essential for the retrograde particle movement of intraflagellar transport (IFT). J Cell Biol 141, 979–992

Pazour GJ, Dickert BL, Witman GB (1999) The DHC1b (DHC2) isoform of cytoplasmic dynein is required for flagellar assembly. J Cell Biol 144, 473–481

Phillips DM, Pilder SH, Olds-Clarke P, Silver LM (1993) Factors that may regulate assembly of the mammalian sperm tail deduced from a mouse *t* complex mutation. Biol Reprod 49, 1347–1352

Pilder SH (1997) Identification and linkage mapping of *Hst7*, a new *M. spretus/M. m. domesticus* Chromosome 17 hybrid sterility locus. Mamm Genome 8, 290–291

Pilder SH, Hammer M, Silver LM (1991) A novel mouse chromosome 17 hybrid sterility locus: implications for the origin of *t* haplotypes. Genetics 129, 237–246

Pilder SH, Decker CL, Islam S, Buck C, Cebra-Thomas JA et al. (1992) Concerted evolution of the Mouse *Tcp10* gene family: implications for the functional basis of *t* haplotype transmission ratio distortion. Genomics 12, 35–41

Pilder SH, Olds-Clarke P, Phillips DM, Silver LM (1993) *Hybrid Sterility 6:* a mouse *t* complex locus controlling sperm flagellar assembly and movement. Dev Biol 159, 631–642

Pilder SH, Olds-Clarke P, Orth JM, Jester WF, Dugan L (1997) *Hst7:* a male sterility mutation perturbing sperm motility, flagellar assembly, and mitochondrial sheath differentiation. J Androl. 18, 663–671

Porter ME (1996) Axonemal dyneins: assembly, organization, and regulation. Curr Opin Cell Biol 8, 10–17

Porter ME, Bower R, Knott JA, Byrd P, Dentler W (1999) Cytoplasmic dynein heavy chain 1b is required for flagellar assembly in *Chlamydomonas.* Mol Biol Cell 10, 693–712

Redkar AA, Olds-Clarke P, Dugan LM, Pilder SH (1998) High-resolution mapping of sperm function defects in the *t* complex fourth inversion. Mamm Genome 9, 825–830

Rosenbaum JL, Cole DG, Diener DR (1999) Intraflagellar transport: the eyes have it. J Cell Biol 144, 385–388

Samant SA, J Fossella, Silver LM, Pilder SH (1999) Mapping and cloning recombinant breakpoints demarcating the *Hybrid Sterility 6*-specific sperm tail assembly defect. Mamm Genome 10, 88–94

Seitz AW, Bennett D (1985) Transmission distortion of *t*-haplotypes is due to interactions between meiotic partners. Nature 313, 143–144

Silver LM (1993) The peculiar journey of a selfish chromosome: mouse *t* haplotypes and meiotic drive. Trends Genet 9, 250–254

Silver LM (1995) *Mouse Genetics.* (New York: Oxford University Press)

Silver LM, Artzt K (1981) Recombination suppression of mouse *t*-haplotypes is due to chromatin mismatching. Nature 290, 68–70

Silver LM, Buck C (1993) The mouse *t* complex distorter-3 (*Tcd-3*) locus and transmission ratio distortion. Genet Res 62, 133–137

Supp DM, Witte DP, Potter SS, Brueckner M (1997) Mutation of an axonemal dynein affects left-right asymmetry in *inversus viscerum* mice. Nature 389, 963–966

Tanaka Y, Zhang Z, Hirokawa N (1995) Identification and molecular evolution of new dynein-like protein sequences in rat brain. J Cell Sci 108, 1883–1893

Ting C-T, Tsaur S-C, Wu M-L, Wu C-I (1998) A rapidly evolving homeobox at the site of a hybrid sterility gene. Science 282, 1501–1504

Vaisberg EA, Grissom PM, Mcintosh JR (1994) Three isoforms of dynein heavy chain expressed in human cells. Mol Biol Cell (Suppl) 5, 285a

Vallee RB, Sheetz MP (1996) Targeting of motor proteins. Science 271, 1539–1544

Vaughan KT, Mikami A, Paschal BM, Holzbaur ELF, Hughes SM et al. (1996) Multiple mouse chromosomal loci for dynein-based motility. Genomics 36, 29–38

Witman GB (1992) Axonemal dyneins. Curr Opin Cell Biol 4, 74–79

Wu C-I, Davis AW (1993) Evolution of postmating reproductive isolation: the composite nature of Haldane's rule and its genetic basis. Am Nat 142, 187–212

Wu C-I, Palopoli MF (1994) Genetics of postmating reproductive isolation in animals. Annu Rev Genet 27, 283–308